A BLISTER TEST FOR CHARACTERIZATION OF PREPREG TACK USING 3D-DIC FULL-FIELD MEASUREMENTS

Bakhshi, N[1]*, and Poursartip, A[1]
[1] Composites Research Network, Department of Materials Engineering, The University of British Columbia, Canada
* Corresponding author (nima@composites.ubc.ca)

Keywords*: Prepreg tack, material characterization*

ABSTRACT

A novel application of a blister test for the characterization of prepreg tack is presented. The full-field deformation of samples is measured using cross-polarized, three-dimensional digital image correlation. Taking advantage of the full-field measurements, a new method of calculating the fracture energy of tack from the blister test data is developed. By taking into account the exact local deformation produced in the sample, the proposed methodology circumvents the common requirement to interpret test results using idealized theories of material deformation. The approach is thus well suited to accommodate unique features and behavior exhibited by as-received prepreg materials. Finally, an experimental dataset is presented and thoroughly discussed.

1 INTRODUCTION

Automated Fiber Placement (AFP) is increasingly used by the aerospace industry to produce high-quality composite parts. Higher productivity, reliability, and repeatability are among the features that have led to AFP's widespread adoption. Moreover, significant resources are being allocated to further technological advancements related to AFP, as well as to develop a fundamental understanding of the physical mechanisms involved in this process.

Defect formation during AFP processing of thermoset prepregs is an undesirable phenomenon [1] that may cause manufacturing delays and scrapping of expensive parts [2]. Several competing mechanisms and properties influence the final layup quality. The primary mechanism resisting the formation of defects is prepreg tack.

Tack is a complex phenomenon generally understood as the force required to separate prepreg from the adherend substrate at their interface, shortly after being brought into contact under light pressure and moderate temperature. Several process parameters influence tack, including layup speed, temperature, and compaction pressure, as well as the geometry over which delamination is occurring. Conceptualizing tack involving separate mechanisms of cohesion (formation of tack) and de-cohesion (separation) is beneficial for illuminating and modeling the effect of fundamental mechanisms involved [3-4].

Different experimental methods have been developed over the past few decades to measure prepreg tack (e.g., the probe test [5] and the peel test [6]). The ASTM standard method (ASTM D8336) of characterizing prepreg tack is the continuous application and peel procedure [7]. In this method, a prepreg sample is placed on a frictionlessly moving tool. A compaction roller applies the desired compaction force onto the prepreg surface and simultaneously guides the prepreg to be peeled off; hence, cohesion and de-cohesion of tack occur in a single stage under the roller.

The blister test method was first introduced by Dannenberg in 1961 [8] and has been an extensive area of research ever since. This method has been primarily applied to measure the adhesion of pressure-sensitive adhesives. Typically, a pressurized fluid is injected into the interface between an adherend and the adhesive to perform the test, while the adhesive film's peak deformation is measured. Using relevant theories of deformation (e.g., plate or membrane theory), the peak value of deformation and internal pressure is connected to the adhesive system's energy release rate.

In the present work, a novel application of the blister test for characterization of prepreg tack is introduced. The prepreg sample's full-field deformation field is measured using cross-polarized, three-dimensional digital image correlation. A new methodology for characterizing the energy release rate of prepreg tack is developed. Using the full-field measurements, theoretical constraints typically imposed on deformation fields are minimized to achieve a more realistic representation of material orthotropy and the samples' local behavior during blister formation and growth.

By applying the blister test method to prepreg materials, cohesion and de-cohesion stages are entirely decoupled, enhancing the level of control over experimental parameters of interest. Layup temperature and compaction pressure can be easily controlled during experiments. Moreover, the effect of different fiber orientations between two adjacent plies on the development of intimate contact, tack formation, and tack resistance during de-cohesion can be investigated. Additionally, dwell-time (i.e., the time elapsed between the application of compaction pressure and delamination) can be controlled. This is of great practical importance as in many manufacturing facilities, composite layups may be stored at room temperature for several hours before proceeding to autoclave processing. Using this method, tack is characterized in a geometry that is potentially more representative of an actual defect growing during the AFP process.

2 Experimental Method

2.1 Material

The Hexcel AS4/8552 unidirectional prepreg system [9] was used to conduct the current experiments. In this study, a single ply of AS4/8552 prepreg was cut into 10 cm x 10 cm square samples. A flat-white random speckle pattern was subsequently applied to the prepreg surface to perform image correlations, further explained in the following section.

2.2 Measurement Methods

The sample's full-field deformations are measured using cross-polarized, three-dimensional digital image correlation (3D-DIC). 3D-DIC is a non-contact optical technique that measures full-field deformations and strains by tracking the position of a spatially unique pattern across multiple image frames.

Typically, matt-black spray paint is used to produce a random speckle pattern against a flat-white background to maximize image contrast [10] and control the light reflected from the sample. Samples prepared according to the conventional coating method were subjected to SEM imaging by Duffner [11]. A total of 100 sections from these SEM Images were analyzed using ImageJ software [12] to measure the thickness of the prepreg layer (average of 216.3 μm) and the background white paint (average of 66.7 μm). An increase of 30.8% in the total sample thickness was observed for samples treated with background paint. Uncured prepreg is highly compliant in out-of-plane bending at the relevant process temperatures. Therefore, the addition of the background paint layer may substantially affect prepreg's flexural rigidity and deformation profile.

To circumvent this issue, the background paint layer was removed, and a flat-white random speckle pattern was directly applied to the prepreg surface. Orthogonal Linear Polarizing filters were used on the light sources and cameras. This imaging technique called cross-polarization improves DIC outcomes [13] by filtering unwanted reflections, increasing contrast, and spatial precision. To perform DIC measurements, polarizing filters were used to polarize the light source horizontally. Specular reflections from the *glossy* prepreg surface preserve the incident light's polarity while diffusive reflections from the flat speckle pattern do not. Vertically oriented polarizing lenses were added to the DIC cameras. The linear polarizing lenses filter out most glossy reflections from the prepreg surface, which prevents saturation of pixels in the image sensors while allowing the light reflected from the speckle pattern to pass through.

DIC cameras were set up above the sample angled slightly inward, so each camera was capturing a similar region of interest; this allows the DIC software to produce three-dimensional reconstructions of the field of view. Time-lapse images were captured and analyzed using Correlated Solutions VIC-Snap and VIC-3D software.

2.3 Experimental Setup

An Aluminum tool containing a through-hole with 1.6 mm (1/16 inch) diameter is used to perform the experiments. The bottom end of the hole is threaded and connected via flexible tubing to a pressure reservoir (Figure 1, a-b). A 10 kPa pressure transducer located immediately below the tool opening measures the pressure inside the blister, while a 100 kPa pressure transducer near the pressure reservoir is used to set the tank pressure at a constant value.

Prior to each experiment, the tool was rigorously cleaned with alcohol to remove any resin residues. A 25 μm thick fluorinated ethylene propylene (FEP) film was cut by a 25 mm diameter circular punch. Then, the FEP layer and prepreg were placed on the tool while their centers were aligned with the center of the hole. The FEP layer placed between the tool and prepreg sample creates a well-defined non-adhesive region for delamination to initiate. A roller was used to apply light pressure on the sample to promote intimate contact and tack formation. Finally, the perimeter of the prepreg sample was bounded with a tacky tap to prevent any potential air leakage.

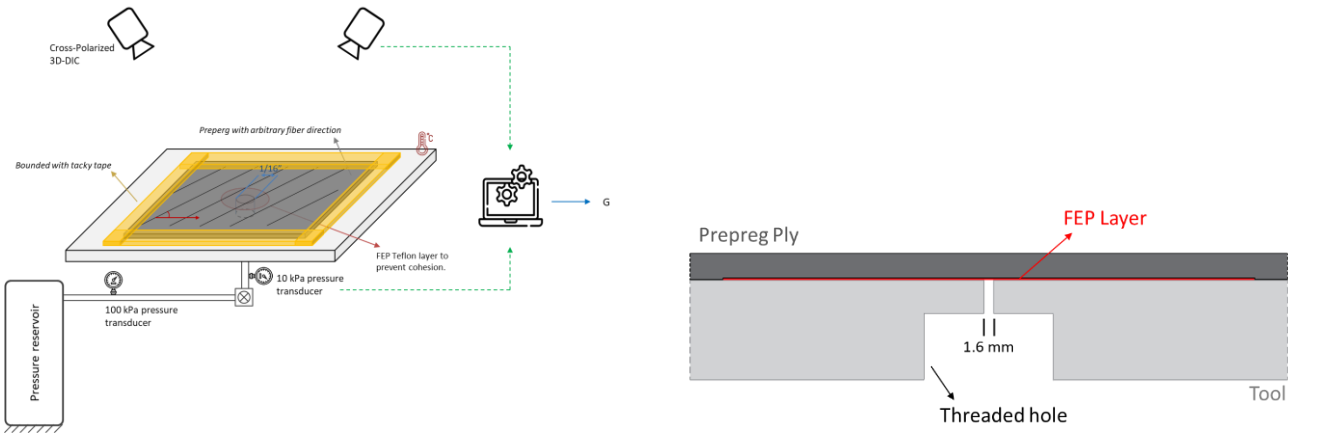

a. Schematic of the experimental setup

b. A schematic cross-section of the experimental tool and sample.

Figure 1. experimental setup.

3 Analysis Method

3.1 Background

Fracture energy or energy release rate measures energy available at the crack front for an increment of crack growth [14]. In blister test experiments, the onset of instability can be detected by a sudden increase in peak deformation of blister and a sudden increase in the delaminated area (see Figure 2). While the test is stable, the fracture energy of tack can be calculated incrementally:

$$G = \frac{1}{\Delta A}(\Delta W_{external} - \Delta U_{internal}) \quad (1)$$

where G is fracture energy, ΔA is the newly generated area over an increment of crack growth, $\Delta W_{external}$ is the change in external work performed on the medium over the incremental crack growth and $\Delta U_{internal}$ is the change in internal energy stored in the blister over the increment of crack growth.

In pressure-sensitive adhesive literature, a closed-form theory of deformation of the film is traditionally implemented to relate the blister geometry to the applied pressure, with the ultimate purpose of finding the energy terms (i.e., $\Delta W_{external}$ and $\Delta U_{internal}$) as a function of the applied pressure (or other control parameters). Elastic membrane [15] and plate [16] theories are used, respectively, for extreme cases of stretching and bending dominant blister deformation. For the intermediate cases, finite element models [17] have been utilized.

The large diameter to thickness ratio observed in blister testing of prepregs indicates that the primary mode of deformation is stretching. Developing a closed-form solution for a nonlinear and orthotropic theory of membrane deformation is non-trivial. Moreover, the combination of rigid fibers embedded in a viscoelastic low-modulus resin in as-received prepregs (i.e., while prepreg is in the pre-gelation stage) prevents the material from deforming as a continuum. The resin may incrementally deform until enough energy is stored to move/deform the considerably stiffer fibers, at which point a larger crack growth occurs. This leads to the blister's non-uniform growth (see Figure 2a), which would manifest itself as an error in any theory attempting to idealize blister geometry or its deformation profile.

The present study uses DIC's full-field measurements to overcome this challenge and avoid imposing assumptions on the deformation fields other than elastic behavior. In the following, a FEM-like discretization approach is developed to directly calculate the fracture energy of tack.

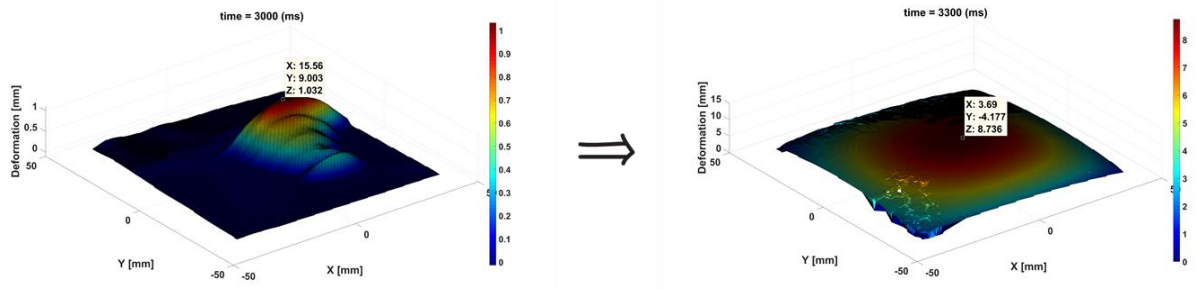

a. Onset of instability b. Unstable blister growth

Figure 2. a: non-uniform delamination of crack, at t=3000 ms (a: onset of instability).
a to b: sudden increase in blister profile and sudden increase in peak deformation from 1.03 mm to 8.74 mm in a ~300 ms-window.

3.2 Blister Boundary Detection

Digital Image Correlation produces a set of elements over the experimental region of interest. Subsequently, the DIC algorithm calculates deformations by correlating the shape of the random speckle pattern within subsets of elements across different picture frames. The final output consists of datasets containing coordinates, deformations, strains, and associated uncertainties. This information is transferred into Matlab for further analysis.

The first step towards analyzing the acquired data is to reliably extract the blister domain out of the whole region of interest on which measurements were performed. This process needs to be automated as much as possible since each experiment involves several image frames, and each frame consists of thousands of data points. Any manual attempt at defining the blister boundary would be too time-consuming, and inconsistencies in manual judgment could lead to erroneous calculations of energy terms.

Clearly, adhesive bonds act as a clamped boundary condition resisting displacement and rotation. An algorithm has been developed to calculate the gradient vector of out-of-plane deformation $(w_{,x}, w_{,y})$ from the DIC point cloud data. Then, the norm of the gradient vector is used for further analysis:

$$g = \|\boldsymbol{\nabla} w\| = \sqrt{(w_{,x})^2 + (w_{,y})^2} \tag{2}$$

where the comma subscript denotes partial differentiation with respect to the independent parameters noted after the comma. The FEP layer creates the initial delaminated area from which the blister grows. Therefore, for each test, some regions can be identified that remain unloaded throughout the experiment (Figure 3). The average out-of-plane deformation and gradient of out-of-plane deformation over these unloaded regions are calculated in each frame to establish the corresponding zero values. Now, the blister domain can be found using the experimentally established zero value.

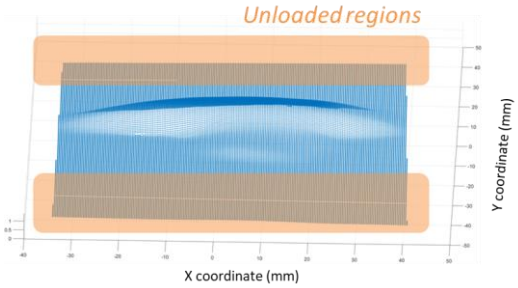

Figure 3. A sample image highlighting unloaded regions in an experiment.

3.3 External Work Calculation

Under constant pressure conditions, the work performed by pressurized gas is $P\Delta V$, where P is the applied pressure, and ΔV is the change in blister volume. Therefore, the calculation of external work is reduced to obtaining the changes in the blister volume from one frame to another.

Triangulation can be produced over the DIC point cloud coordinates wherein each node's position, deformations, and strains are known (Figure 4). Having the coordinates of each element's nodes, the area of each triangular element is calculated. The element volume is obtained by using the average out-of-plane deformation of all three nodes and the element area. Finally, each frame's blister volume and delaminated area are found by summing the elemental areas and volumes over all elements. The change in the delaminated area between adjacent frames is the newly generated area ΔA, required for the calculation of G.

3.4 Internal Energy Calculation

Part of the external work supplied by pressurized gas is stored in the deformed body of prepreg. As mentioned earlier, in a typical blister test, this energy is estimated through theories of membrane or plate deformation. Here, we propose a new approach to directly calculate the strain energy from full-field deformations experimentally measured via Digital Image Correlation (DIC). Total strain energy reads:

$$U = \frac{1}{2}\int_V \sigma_{ij}\,\varepsilon_{ij}\,\mathrm{d}V = \frac{1}{2}h\left[Q_{11}\int_\Omega \varepsilon_{11}^2\,\mathrm{d}\Omega + 2Q_{12}\int_\Omega \varepsilon_{11}\varepsilon_{22}\,\mathrm{d}\Omega + Q_{22}\int_\Omega \varepsilon_{22}^2\,\mathrm{d}\Omega + Q_{66}\int_\Omega \gamma_{66}^2\,\mathrm{d}\Omega\right] \tag{3}$$

where Q_{ij} are components of the on-axis stiffness matrix of the prepreg ply. Strain energy is a non-negative scalar value. Therefore, the integration over the whole blister domain is equivalent to the summation of integrations over smaller elements for all elements.

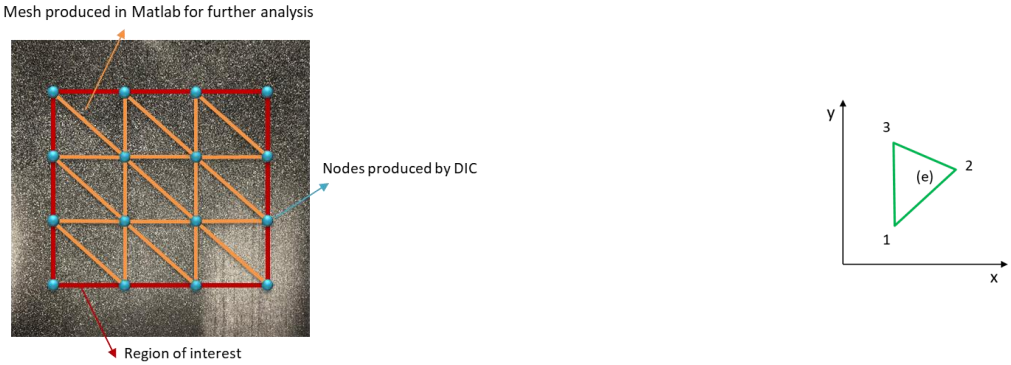

a. b.

Figure 4. a: Flat-white random speckle pattern applied on a sample of as-received prepreg. A schematic of DIC nodes and resulting triangulations over an arbitrary region of interest is imposed on the prepreg's image. b: An arbitrary element with known coordinates, deformations, and strains, observed in the physical coordinate system.

$$U = \frac{1}{2}h\sum_{e=1}^{N}\int_{\Omega^{(\mathrm{e})}} U_0^{(e)}\,\mathrm{d}\Omega, \qquad \Omega = \bigcup_{e=1}^{N}\Omega^{(e)} \tag{4}$$

$$U = \frac{1}{2}h\left[Q_{11}\sum_{e=1}^{N}\int_{\Omega^{(\mathrm{e})}}\left(\varepsilon_{11}^{(e)}\right)^2\mathrm{d}\Omega + 2Q_{12}\sum_{e=1}^{N}\int_{\Omega^{(\mathrm{e})}}\left(\varepsilon_{11}^{(e)}\varepsilon_{22}^{(e)}\right)\mathrm{d}\Omega + Q_{22}\sum_{e=1}^{N}\int_{\Omega^{(\mathrm{e})}}\left(\varepsilon_{22}^{(e)}\right)^2\mathrm{d}\Omega + Q_{66}\sum_{e=1}^{N}\int_{\Omega^{(\mathrm{e})}}\left(\gamma_{66}^{(e)}\right)^2\mathrm{d}\Omega\right] \tag{5}$$

Note that the nodal strain values are known while the strain distribution in each element is unknown. Given that the DIC elements are sufficiently small, each component of strain can be considered to vary linearly over an element:

$$\varepsilon_{ij,n}^{(e)} = \alpha_0 + \alpha_1 x_\mathrm{n} + \alpha_2 y_\mathrm{n} \tag{6}$$

where $n = 1, 2, 3$ is the node number in element (e). The system of equations to be solved for each element reads:

$$\begin{bmatrix}1 & x_1 & y_1\\ 1 & x_2 & y_2\\ 1 & x_3 & y_3\end{bmatrix}\begin{Bmatrix}\alpha_0\\ \alpha_1\\ \alpha_2\end{Bmatrix} = \begin{Bmatrix}\varepsilon_{ij,1}\\ \varepsilon_{ij,2}\\ \varepsilon_{ij,3}\end{Bmatrix} \rightarrow \begin{Bmatrix}\alpha_0\\ \alpha_1\\ \alpha_2\end{Bmatrix} = \begin{bmatrix}1 & x_1 & y_1\\ 1 & x_2 & y_2\\ 1 & x_3 & y_3\end{bmatrix}^{-1}\begin{Bmatrix}\varepsilon_{ij,1}\\ \varepsilon_{ij,2}\\ \varepsilon_{ij,3}\end{Bmatrix} \tag{7}$$

In the matrix format, introducing $\{d\}$ as the vector of nodal values of strains, equation (7) can be rearranged as $\{\alpha\} = [M]^{-1}\{d\}$. Finally, the strain components used to evaluate equation (5) are found. Energy density is integrated over triangular elements using the Gauss quadrature method [18].

$$\varepsilon_{ij}^{(e)}(x, y) = [1 \quad x \quad y][M]^{-1}\{d\} \tag{8}$$

4 Results and Discussions

Residual stresses are induced in the AFP process due to tensions applied throughout the delivery system and by conforming prepreg tows onto arbitrary layup paths. These residual stresses are the primary source contributing to the formation and growth of layup defects. The inherent variability of prepreg materials [19-21] can make the material system prone to the initiation of small defects. On the other hand, stable crack growth is a fundamentally incremental process. Therefore, even small residual stresses can potentially result in the appearance of defects in the final layup. As a result of this argument, for this initial demonstration, blister growth under constant loading is studied.

In the following, a set of experimental results are presented to demonstrate the applicability and relevance of developed methods. A prepreg sample was prepared according to the protocol described in section 2. Subsequently, the sample was laid down on the tool using a light pressure applied through a compaction roller. The experiment was performed at room temperature (25.4 ^{o}C) while the blister was subjected to 5.9 kPa pressurized air.

Raw deformation profiles produced by the digital image correlation software are presented in Figure 5. It is of interest to note that X-axis is along the fiber direction. For the first 3000 ms, the blister grows gradually, which is evident in the small growth of the delaminated area as well as the incremental rise of peak out-of-plane deformation (tagged in each image). The 3000 ms time, however, marks the onset of instability for this specific experiment. At this point, in less than 300 ms, the blister experiences an ~8.5-fold increase in peak deformation and devours all the areas of interest monitored by the DIC software.

The constant air pressure throughout the experiment does not mean the force available at the crack front for extending the crack perimeter is constant. Typically, in blister experiments, the energy release rate, G, has a superlinear relationship with the diameter of the delaminated area. Therefore, as the blister grows, the force available for advancing the crack front increases, eventually leading to instability of the system.

The methodology developed in previous sections was applied to the first 1800 ms (or 6 image frames) to extract the fracture energy of tack. The result is presented in Figure 6. The sudden rise in frame 4 can be understood by considering the discrete nature of deformation measurements: large delamination occurs from frames 2 to 3 while the area change remains relatively small from frames 3 to 4 (note $G \propto 1/\Delta A$). A higher frequency image acquisition system can provide a smoother and more gradual ΔA progression, which helps in producing more data points thus avoiding the step-wise change in ΔA. This will further enhance measurement quality.

There is no published information on the tack of AS4/8552. However, Wohl et al. [5] have extensively studied the tack of IM7/8552-1 by the probe test method. A histogram (Figure 7) of the fracture energies for the experiments performed at room temperature is constructed from data published in [5]. A wide range of measured values is observed due to different humidity, rate, probe size, and contact time. However, more than half of the measured fracture toughness values are below 5 J/m^{2,} consistent with the experimental results of the present work.

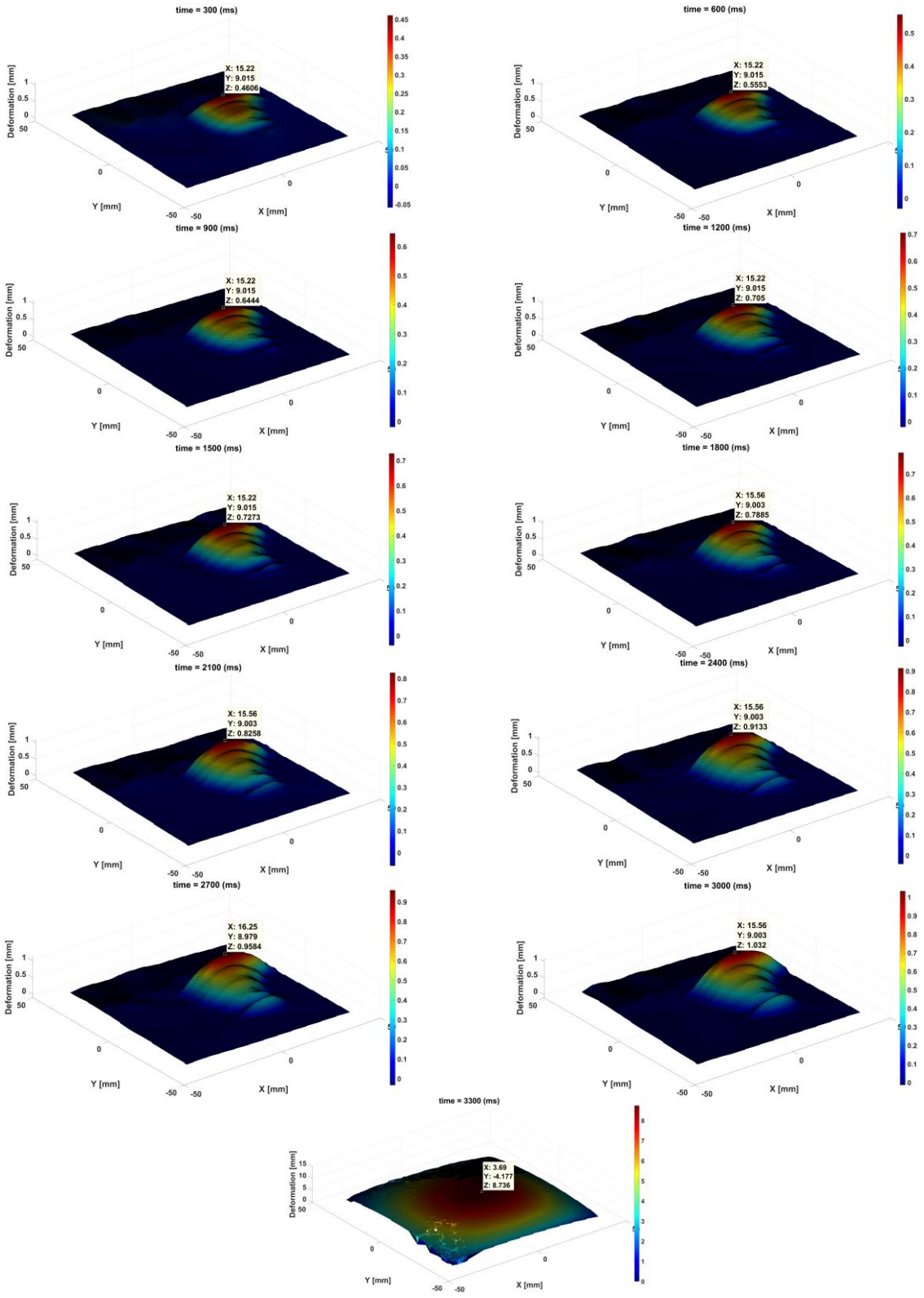
time = 300 (ms)
X: 15.22
Y: 9.015
Z: 0.4606
time = 600 (ms)
X: 15.22
Y: 9.015
Z: 0.5553
time = 900 (ms)
X: 15.22
Y: 9.015
Z: 0.6444
time = 1200 (ms)
X: 15.22
Y: 9.015
Z: 0.705
time = 1500 (ms)
X: 15.22
Y: 9.015
Z: 0.7273
time = 1800 (ms)
X: 15.56
Y: 9.003
Z: 0.7885
time = 2100 (ms)
X: 15.56
Y: 9.003
Z: 0.8258
time = 2400 (ms)
X: 15.56
Y: 9.003
Z: 0.9133
time = 2700 (ms)
X: 16.25
Y: 8.979
Z: 0.9584
time = 3000 (ms)
X: 15.56
Y: 9.003
Z: 1.032
time = 3300 (ms)
X: 3.69
Y: -4.177
Z: 8.736
Deformation [mm]
Y [mm]
X [mm]

Figure 5. Progression of blister test with 300 ms time intervals.

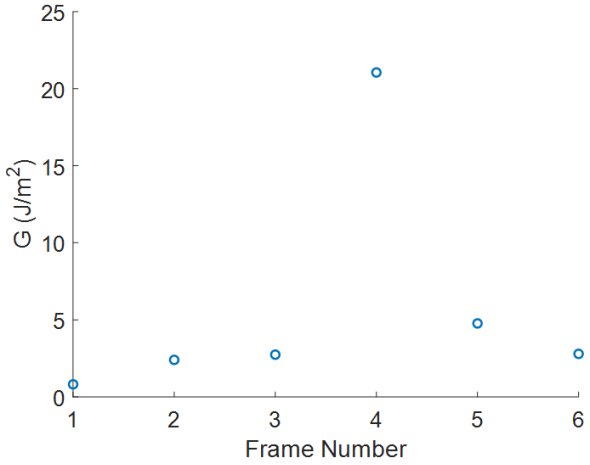

Figure 6. Fracture energies obtained from a test performed at room temperature while the sample was subjected to 5.9 kPa pressure.

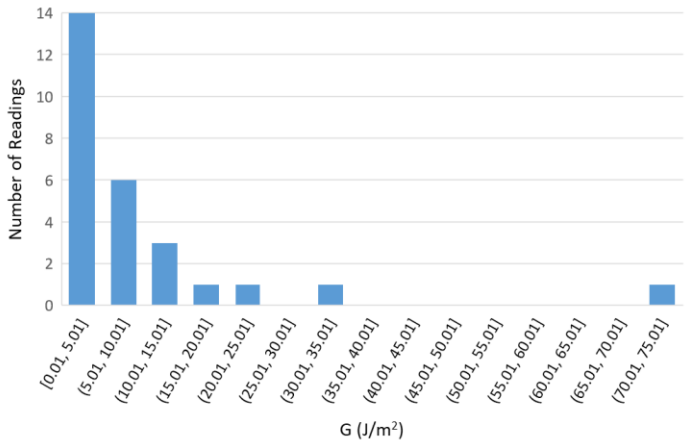

Figure 7. Histogram of room temperature tack measurements performed with various experimental parameters, constructed using data published in [5].

5 Concluding Remarks

Automated Fiber Placement is a rapidly developing technology used in the aerospace industry to laminate expensive, large, and complex parts. Despite its many advantages, the appearance of process-induced defects is one of the most critical challenges facing AFP processing, hindering productivity and cost-effectiveness. Prepreg tack is the primary mechanism that resists the formation of defects in AFP. A blister test methodology inspired by the existing literature on pressure-sensitive adhesives has been developed to characterize prepreg tack. The proposed method decouples the formation of tack (cohesion stage) and delamination (de-cohesion stage) in which the mechanical resistance of tack is manifested. This decoupling grants further control over experimental parameters relevant to AFP processing, including the time elapsed from AFP processing to autoclave processing.

Three-dimensional Digital Image Correlation was performed to obtain full-field measurements of prepreg deformation. A novel approach was developed to process the additional deformation data captured through DIC, which enabled a direct calculation of fracture energy of tack. This new approach couples experimental DIC measurements with finite element discretized formulations to calculate the energy terms required to obtain the tack fracture energy. An experimental data set is disclosed to demonstrate the application of this method. The results were compared to the existing literature to show the relevance of the methodology. Future efforts will focus on fully characterizing the dependence of tack on the underlying substrate (or prepreg orientation) and layup parameters (e.g., temperature, compaction force, dwell time, etc.), as well as blister method parameters such as blister internal pressure, tool opening size, and FEP layer characteristics.

Acknowledgments

Authors gratefully acknowledge financial support from the Composites Research Network (CRN). We would like to acknowledge discussions with colleagues at the Composites Research Network (CRN), as well as Dr. Alireza Forghani,

Malcolm Lane, and Paulo Silva at Convergent Manufacturing Technologies. We would like to thank Malcolm Lane for his assistance with the development of the experimental setup.

6 REFERENCES

[1] N. Bakhshi and M. Hojjati, “An experimental and simulative study on the defects appeared during tow steering in automated fiber placement”. *Composites Part A: Applied Science and Manufacturing*, Vol. 113pp. 122–131, 2018.

[2] P. Silva, M. Lane, J. McRoberts, A. Forghani, A. Poursartip, S. Hind, M. Rahmat, D. Djokic and A. Yousefpour, “Simulation of Deposition Manufacturing Processes of Polymer Matrix Composites”. *The NAFEMS World Congress*, 2019.

[3] A. Forghani, C. Hickmott, H. Bedayat, C. Wohl, B. Grimsley, B. Coxon and A. Poursartip, “A Physics-Based Modelling Framework for Simulation of Prepreg Tack in AFP”. *The Society for the Advancement of Material and Process Engineering*, 2017.

[4] A. Forghani, C. Hickmott, V. Hutten, H. Bedayat, C. Wohl, B. Grimsley, B. Coxon and A. Poursartip, “Experimental Calibration of a Numerical Model of Prepreg Tack for Predicting AFP Process Related Defects”. *The Society for the Advancement of Material and Process Engineering*, 2018.

[5] C. Wohl, F. Palmieri, A. Forghani, C. Hickmott, H. Bedayat, B. Coxon, A. Poursartip and B. Grimsley “Tack measurements of prepreg tape at variable temperature and humidity”. *The Composites and Advanced Materials Expo*, 2017.

[6] R. Crossley, P. Schubel, and N. Warrior, “The experimental determination of prepreg tack and dynamic stiffness”. *Composites Part A: Applied Science and Manufacturing*, Vol. 43, No. 3, pp. 423–434, 2012.

[7] ASTM D8336-21, “Standard Test Method for Characterizing Tack of Prepregs Using a Continuous Application-and-Peel Procedure”. 2021.

[8] H. Dannenberg, “Measurement of adhesion by a blister method”. *Journal of Applied Polymer Science*, Vol. 5, No. 14, pp. 125–134, 1961.

[9] HEXCEL, “HexPly® 8552 Product Data Sheet”. . 2016.

[10] W. LePage, J. Shaw, and S. Daly, “Optimum paint sequence for speckle patterns in digital image correlation”. *Experimental Techniques*, Vol. 41, No. 5, pp. 557–563, 2017.

[11] C. Duffner, “Experimental study of the pre-gelation behaviour of composite prepreg”. , 2019.

[12] W. S. Rasband, “U. S. National Institutes of Health, Bethesda, Maryland, USA, https://imagej.nih.gov/ij/”. . 2018 1997.

[13] W. S. LePage, S. H. Daly, and J. A. Shaw, “Cross polarization for improved digital image correlation”. *Experimental Mechanics*, Vol. 56, No. 6, pp. 969–985, 2016.

[14] T. L. Anderson, *Fracture mechanics: fundamentals and applications*. CRC press, 2017.

[15] A. Gent and L. Lewandowski, “Blow-off pressures for adhering layers”. *Journal of applied polymer science*, Vol. 33, No. 5, pp. 1567–1577, 1987.

[16] J. Hinkley, “A blister test for adhesion of polymer films to SiO2”. *The Journal of Adhesion*, Vol. 16, No. 2, pp. 115–125, 1983.

[17] K. Mahan, D. Rosen, and B. Han, “Blister testing for adhesion strength measurement of polymer films subjected to environmental conditions”. *Journal of Electronic Packaging*, Vol. 138, No. 4, 2016.

[18] J. Fish and T. Belytschko, *A first course in finite elements*. Wiley, 2007.

[19] A. L. Stewart and A. Poursartip, “Characterization of fibre alignment in as-received aerospace grade unidirectional prepreg”. *Composites Part A: Applied Science and Manufacturing*, Vol. 112pp. 239–249, 2018.

[21] K. Potter, “Understanding the origins of defects and variability in composites manufacture”. pp. 18–25, 2009.